Pergamon

Int. J. Solids Structures Vol. 32, No. 24, pp. 3555–3571, 1995

0020–7683/95 $9.50 + .00

0020–7683(95)00015–1

A SINGLE-REGION TIME DOMAIN BEM FOR DYNAMIC CRACK PROBLEMS

P. FEDELINSKI† and M. H. ALIABADI

Wessex Institute of Technology, University of Portsmouth, Ashurst Lodge, Ashurst, Southampton, SO40 7AA, U.K.

and

D. P. ROOKE

Defence Research Agency, Farnborough, Hants GU14 6TD, U.K.

(*Received* 20 *August* 1994; *in revised form* 10 *February* 1995)

Abstract – A time domain boundary element method, which allows the analysis of dynamic crack problems by using a single-region formulation, is presented. The present method generates the distinct set of boundary integral equations by applying the displacement equation to one of the crack surfaces and the traction equation to the other. The boundary of the structure is divided into continuous, semi-discontinuous and discontinuous quadratic elements. The temporal variation of boundary displacements and tractions is approximated by piecewise linear and constant functions, respectively. The dynamic stress intensity factors are calculated using the crack opening displacements and the path independent $\tilde{J}$-integral. This method is used to study dynamic behaviour of stationary cracks in finite and infinite domains in two-dimensional analysis. The results for two examples are compared with other reported solutions, showing good agreement.

1. INTRODUCTION

The aim of dynamic fracture mechanics [see e.g. Sih (1977); Freund (1990)] is to analyse the growth, arrest and branching of moving cracks in structures subjected to dynamic loads. The stress field in the vicinity of the crack is usually characterized by dynamic stress intensity factors (DSIFs) which, for transient problems, are functions of time. Structures with arbitrary shape and time-dependent boundary conditions need to be analysed by numerical methods. The boundary element method (BEM) has been successfully applied to stationary and growing cracks in infinite and finite domains. Solutions in dynamics using the BEM are usually obtained [see e.g. Manolis and Beskos (1988); Dominguez (1993)] by either the time domain method, Laplace or Fourier transforms or the dual reciprocity method.

The application of the time domain method in fracture mechanics has been reported in many papers.

Nishimura *et al.* (1987, 1988) used the double layer potentials. The boundary integral equations in this formulation contain hypersingular integrals. The equations were regularized by using integration by parts twice. The spatially constant and temporally linear shape functions were used for approximation. The crack opening displacements (CODs) were fitted with an interpolation function, which was then used to calculate the DSIF. The method was applied for stationary and growing straight cracks in 2D, and plane cracks in 3D infinite domains. Zhang and Achenbach (1989) used a different regularization procedure from Nishimura *et al.* (1987, 1988). They used constant elements away from the crack front and spatial square-root functions near the crack tip. A linear time-variation was used. The method was applied for collinear cracks in the infinite domain. Zhang and Gross (1993) used the two-state conservation integral of elastodynamics, which leads to non-hypersingular traction boundary integral equations. The unknown quantities in this approach

†On leave from Silesian Technical University of Gliwice, Poland.

are the crack opening displacements and their derivatives. Similar time and space discretization was used. The method was applied to penny-shaped and square cracks in the infinite domains. Hirose (1989) and Hirose and Achenbach (1988, 1989, 1991) used the formulation based on the traction equation. Piecewise linear temporal functions were used and the COD was interpolated using the analytical solution of the static problem. The method was applied for both stationary and growing penny-shaped cracks.

Nicholson and Mettu (1988) and Mettu and Nicholson (1988) used two types of approximation: (i) constant elements for spatial and temporal interpolation of boundary quantities; and (ii) quadratic in space and linear in time. The DSIFs were determined using the COD. The method was applied to solve several opening-mode crack problems, namely an infinite plate containing either a semi-infinite or a finite crack subjected to crack face loading and a centre-cracked finite plate subjected to a sudden remote tensile stress. Dominquez and Gallego (1992) used a mixed variation of boundary values in which tractions were assumed to be constant and displacements linear in time. The boundaries were divided into quadratic elements. At the crack tips ordinary and traction-singular quarter-point elements (QPEs) were used. The DSIFs were determined using the COD and tractions of the traction-singular elements. The method was applied to finite bodies with cracks. Mixed-mode crack problems were analysed using the subregion technique. Gallego and Dominguez (1992) modelled the crack growth by using moving singular elements and a remeshing technique. The method was applied for problems for which the motion of the crack tip was fully specified: a semi-infinite crack that grew at the constant speed in an unbounded domain and a finite length crack in a finite plane body. Mettu and Kim (1991) used the superposition of two stationary crack problems. The constant approximation in time and space was used. The DSIFs were calculated using the COD and a least-squares minimization. The method was applied to the problem of growth of a semi-infinite crack in the infinite domain subjected to crack-face loading.

The solution of a general crack problem cannot be achieved in a single-region analysis by the direct application of the BEM, because the coincidence of crack nodes gives rise to a singular system of algebraic equations. The boundary integral equations for two coincident points on both surfaces of the crack are identical, because they have the same coordinates, and integrals are calculated along the same boundary. Recently, Portela *et al.* (1992, 1993) applied the so-called dual boundary element method (DBEM) to stationary and growing cracks in two-dimensional analysis. A non-singular system of equations was obtained by using two different boundary integral equations for coincident points, i.e. the displacement and traction equation. The unknown absolute values of displacements and tractions along the crack surfaces and others boundaries of the body are obtained directly by the solution of the system of equations. This method was extended later by Mi and Aliabadi (1992, 1994) to stationary and growing cracks in three-dimensional analysis. Fedelinski *et al.* (1993, 1994a) presented an application of the DBEM combined with the dual reciprocity method for stationary cracks in structures subjected to dynamic loading.

In this paper the DBEM and the time domain method are presented. Preliminary results of this approach were presented in Fedelinski *et al.* (1994b, 1994c). The displacement and the traction boundary integral equations are formulated. The discretized form of the equations is obtained by dividing the boundary into quadratic elements and using a time-stepping procedure. The formulae for analytical temporal integration of the fundamental solutions for linear interpolation of displacements and constant interpolation of tractions are given. The singularities of the fundamental solutions are discussed and the semi-analytical method of spatial integration for the traction equation is described. The DSIFs are calculated using both the crack opening displacements and the path independent $\hat{J}$-integral. To illustrate the possibilities of the method, it is applied to four dynamic crack problems.

2. DUAL BOUNDARY INTEGRAL EQUATIONS AND TIME DOMAIN FORMULATION

Consider a linear, elastic, homogeneous and isotropic body enclosed by a boundary Γ. For a body which is not subjected to body forces and which has zero initial displacements

and velocities, the displacement of a point $\mathbf{x}'$ can be represented by the following boundary integral equation:

$$c_{ij}(\mathbf{x}')u_j(\mathbf{x}', t) = \int_0^t \left[\int_\Gamma U_{ij}(\mathbf{x}', t; x, \tau) t_j(x, \tau)\, d\Gamma(x) \right] d\tau - \int_0^t \left[\int_\Gamma T_{ij}(\mathbf{x}', t; x, \tau) u_j(x, \tau)\, d\Gamma(x) \right] d\tau, \quad i,j = 1,2, \quad (1)$$

where $U_{ij}(\mathbf{x}', t; x, \tau)$, $T_{ij}(\mathbf{x}', t; x, \tau)$ are fundamental solutions of elastodynamics for the displacement equation; $u_j(x, \tau)$, $t_j(x, \tau)$ are displacements and tractions respectively, at the boundary; $c_{ij}(\mathbf{x}')$ is a constant which depends on the position of the collocation point $\mathbf{x}'$; x is a boundary point; t is the time of observation. The summation convention is used for the repeated subscripts.

The traction equation is obtained by differentiating the displacement equation, applying Hooke's law and multiplying by the outward normal at the collocation point. For a point which belongs to the smooth boundary the traction equation is

$$\tfrac{1}{2} t_j(\mathbf{x}', t) = n_i(\mathbf{x}') \left\{ \int_0^t \left[\int_\Gamma U_{kij}(\mathbf{x}', t; x, \tau) t_k(x, \tau)\, d\Gamma(x) \right] d\tau - \int_0^t \left[\int_\Gamma T_{kij}(\mathbf{x}', t; x, \tau) u_k(x, \tau)\, d\Gamma(x) \right] d\tau \right\}, \quad i,j,k = 1,2, \quad (2)$$

where $n_i(\mathbf{x}')$ are components of the outward normal at the collocation point $\mathbf{x}'$, $U_{kij}(\mathbf{x}', t; x, \tau)$ and $T_{kij}(\mathbf{x}', t; x, \tau)$ are fundamental solutions of elastodynamics for the traction equation.

3. NUMERICAL FORMULATION

3.1. *Approximation of boundary displacements and tractions*

The numerical solution of a general mixed-mode crack problem is obtained after discretizing both space and time variations. The boundary Γ of the body is divided into M boundary elements with P nodes per element. The observation time t is divided into N time steps. The temporal variation of boundary quantities is specified by Q values within the time step. Displacements and tractions are approximated within each element using interpolation functions $N^p(\xi)$, and within each time step using interpolation functions $M^q(\tau)$. The boundary integral equations are applied for all the nodes of the boundary elements. After the approximation, the displacement and the traction equations are

$$c_{ij}^l u_j^{lN} = \sum_{m=1}^{M} \sum_{p=1}^{P} \sum_{n=1}^{N} \sum_{q=1}^{Q} \left\{ t_j^{mpnq} \int_{-1}^{1} \left[\int_{\tau^{n-1}}^{\tau^n} U_{ij}^{lN}(\xi, \tau) M^q(\tau)\, d\tau \right] N^p(\xi) J^m(\xi)\, d\xi - u_j^{mpnq} \int_{-1}^{1} \left[\int_{\tau^{n-1}}^{\tau^n} T_{ij}^{lN}(\xi, \tau) M^q(\tau)\, d\tau \right] N^p(\xi) J^m(\xi)\, d\xi \right\}, l = 1, 2, \ldots, L_1 \quad (3)$$

and

$$\tfrac{1}{2} t_j^{lN} = n_i^l \sum_{m=1}^{M} \sum_{p=1}^{P} \sum_{n=1}^{N} \sum_{q=1}^{Q} \left\{ t_k^{mpnq} \int_{-1}^{1} \left[\int_{\tau^{n-1}}^{\tau^n} U_{kij}^{lN}(\xi, \tau) M^q(\tau)\, d\tau \right] N^p(\xi) J^m(\xi)\, d\xi - u_k^{mpnq} \int_{-1}^{1} \left[\int_{\tau^{n-1}}^{\tau^n} T_{kij}^{lN}(\xi, \tau) M^q(\tau)\, d\tau \right] N^p(\xi) J^m(\xi)\, d\xi \right\}, l = 1, 2, \ldots, L_2, \quad (4)$$

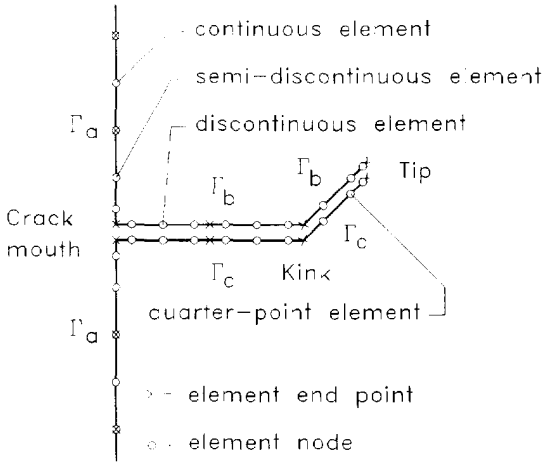

Fig. 1. Modelling of the boundary.

where L_1 and L_2 are respectively the numbers of collocation points for which the displacement and the traction equations are applied; $L_1 + L_2 = L$, the total number of nodes; J^n is the Jacobian and ξ is the local coordinate ($-1 \leqslant \xi \leqslant 1$). A distinct set of boundary integral equations is obtained by applying the displacement equation (3) for collocation points along the external boundary Γ_a and along one of the crack faces Γ_b, and the traction equation (4) for the opposite surface of the crack Γ_c (see Fig. 1).

Quadratic elements are used for the discretization of the boundary. The displacements and tractions are interpolated using: continuous elements for the external boundary Γ_a, semi-discontinuous elements at junctions with the cracks and straight discontinuous elements on the crack faces Γ_b and Γ_c. The geometry is approximated by using continuous elements. The expressions defining the spatial shape functions are given in Table 1, where ξ' is the local coordinate of the node.

The displacements are approximated within each time step by using linear interpolating functions and the tractions are piecewise constant. This mixed variation gives [see Dominguez (1993)] a better solution when the structure is subjected to impact loads. The constant temporal shape function is

$$M^1(\tau) = 1 \tag{5}$$

and the linear temporal shape functions are:

$$M^1(\tau) = \frac{\tau - \tau^{n-1}}{\Delta\tau} \quad \text{and} \quad M^2(\tau) = \frac{\tau^n - \tau}{\Delta\tau}, \tag{6}$$

where $\tau^{n-1} \leqslant \tau \leqslant \tau^n$, $\Delta\tau$ is the time step ($\tau^n = n\Delta\tau$) and the superscripts 1, 2 denote the forward and the backward local time node, respectively.

Table 1. Spatial shape functions

Element	Coordinates ξ'			Spatial shape functions		
	node 1	node 2	node 3	N^1	N^2	N^3
continuous	-1	0	1	$\frac{1}{2}\xi(\xi-1)$	$(1+\xi)(1-\xi)$	$\frac{1}{2}\xi(\xi+1)$
semi-discontinuous	$-\frac{2}{3}$	0	1	$\frac{9}{10}\xi(\xi-1)$	$\frac{3}{2}(\frac{2}{3}+\xi)(1-\xi)$	$\frac{3}{5}\xi(\xi+\frac{2}{3})$
	-1	0	$\frac{2}{3}$	$\frac{3}{5}\xi(\xi-\frac{2}{3})$	$\frac{3}{2}(1+\xi)(\frac{2}{3}-\xi)$	$\frac{9}{10}\xi(\xi+1)$
discontinuous	$-\frac{2}{3}$	0	$\frac{2}{3}$	$\frac{9}{8}\xi(\xi-\frac{2}{3})$	$\frac{9}{4}(\frac{2}{3}+\xi)(\frac{2}{3}-\xi)$	$\frac{9}{8}\xi(\xi+\frac{2}{3})$

3.2. *Evaluation of the time integrals*

The time integrals in eqns (3) and (4) with the simple temporal shape functions in eqns (5) and (6) can be calculated analytically. The following simplifying notation is used:

$$\varphi_\alpha = \frac{R}{c_\alpha \Delta\tau(N-n+1)}, \tag{7}$$

$$\chi_\alpha = \frac{R}{c_\alpha \Delta\tau(N-n)} \tag{8}$$

and

$$\psi_\alpha = \frac{R}{c_\alpha \Delta\tau(N-n-1)}, \tag{9}$$

where c_α is the velocity of the wave; the subscript α denotes the number of the wave, that is $\alpha = 1$ corresponds to the longitudinal and $\alpha = 2$ to the shear wave; R is the distance from the source to a field point.

For the piecewise constant interpolation of tractions the convoluted fundamental solution $\tilde{U}_{ij}^{Nn}$, required in eqn (3), has the form [see Dominguez (1993)]:

$$\tilde{U}_{ij}^{Nn} = \int_{\tau^{n-1}}^{\tau^n} U_{ij}\,\mathrm{d}\tau = \sum_{\alpha=1}^{2} \frac{1}{4\pi\rho c_\alpha^2}\left[\delta_{ij}\left(\ln\frac{1+\sqrt{1-\varphi_\alpha^2}}{\varphi_\alpha} - \ln\frac{1+\sqrt{1-\chi_\alpha^2}}{\chi_\alpha}\right)\right.$$
$$\left. + (-1)^\alpha(\delta_{ij} - 2R_{,i}R_{,j})\left(\frac{\sqrt{1-\varphi_\alpha^2}}{\varphi_\alpha^2} - \frac{\sqrt{1-\chi_\alpha^2}}{\chi_\alpha^2}\right)\right], \tag{10}$$

where ρ is the mass density; δ_{ij} is the Kronecker delta and the index preceded by a comma denotes the derivative with respect to the coordinate.

For the piecewise linear interpolation of displacements the convoluted fundamental solution $\tilde{T}_{ij}^{Nn}$ has the form [see Israil and Banerjee (1990)]:

$$\tilde{T}_{ij}^{Nn} = \int_{\tau^{n-1}}^{\tau^n} T_{ij}M^1\,\mathrm{d}\tau + \int_{\tau^n}^{\tau^{n+1}} T_{ij}M^2\,\mathrm{d}\tau$$
$$= \sum_{\alpha=1}^{2} \frac{\mu}{2\pi\rho c_\alpha^2}\frac{1}{c_\alpha\Delta\tau}\left\{\frac{2A_\alpha}{3}\left[\frac{(1-\varphi_\alpha^2)^{3/2}}{\varphi_\alpha^3} - 2\frac{(1-\chi_\alpha^2)^{3/2}}{\chi_\alpha^3} + \frac{(1-\psi_\alpha^2)^{3/2}}{\psi_\alpha^3}\right]\right.$$
$$\left. - B_\alpha\left[\frac{\sqrt{1-\varphi_\alpha^2}}{\varphi_\alpha} - 2\frac{\sqrt{1-\chi_\alpha^2}}{\chi_\alpha} + \frac{\sqrt{1-\psi_\alpha^2}}{\psi_\alpha}\right]\right\}, \tag{11}$$

where μ is the shear modulus. The coefficients A_α and B_α are given in Appendix A. For the linear interpolation functions the contribution of the integration over the time interval before and after the time node is taken into account.

For the piecewise constant interpolation of tractions the convoluted fundamental solution $\tilde{U}_{kij}^{Nn}$, required in eqn (4), has the form:

$$\tilde{U}_{kij}^{Nn} = \int_{\tau^{n-1}}^{\tau^n} U_{kij}\,\mathrm{d}\tau =$$

$$\sum_{\alpha=1}^{2} \frac{(-1)^{\alpha}\mu}{2\pi\rho c_{\alpha}^2}\,\frac{1}{R}\left\{-C_{\alpha}\left[\frac{1}{\sqrt{1-\varphi_{\alpha}^2}}-\frac{1}{\sqrt{1-\chi_{\alpha}^2}}\right]+2D\left[\frac{\sqrt{1-\varphi_{\alpha}^2}}{\varphi_{\alpha}^2}-\frac{\sqrt{1-\chi_{\alpha}^2}}{\chi_{\alpha}^2}\right]\right\}. \tag{12}$$

The coefficients C_α and D are given in Appendix A.

For the piecewise linear interpolation of displacements the convoluted fundamental solution $\tilde{T}_{kij}^{Nn}$ has the form [see Israil and Banerjee (1991)]:

$$\tilde{T}_{kij}^{Nn} = \int_{\tau^{n-1}}^{\tau^n} T_{kij}M^1\,\mathrm{d}\tau + \int_{\tau^n}^{\tau^{n+1}} T_{kij}M^2\,\mathrm{d}\tau$$

$$= \sum_{\alpha=1}^{2} \frac{(-1)^{\alpha}\mu^2}{2\pi\rho c_{\alpha}^2}\,\frac{1}{Rc_{\alpha}\Delta\tau}\left\{2(E_{\alpha}+F_{\alpha})\left[\frac{\sqrt{1-\varphi_{\alpha}^2}}{\varphi_{\alpha}}-2\frac{\sqrt{1-\chi_{\alpha}^2}}{\chi_{\alpha}}+\frac{\sqrt{1-\psi_{\alpha}^2}}{\psi_{\alpha}}\right]\right.$$

$$-\tfrac{4}{3}G\left[\frac{(1-\varphi_{\alpha}^2)^{3/2}}{\varphi_{\alpha}^3}-2\frac{(1-\chi_{\alpha}^2)^{3/2}}{\chi_{\alpha}^3}+\frac{(1-\psi_{\alpha}^2)^{3/2}}{\psi_{\alpha}^3}\right]$$

$$\left.+E_{\alpha}\left[\frac{\varphi_{\alpha}}{\sqrt{1-\varphi_{\alpha}^2}}-2\frac{\chi_{\alpha}}{\sqrt{1-\chi_{\alpha}^2}}+\frac{\psi_{\alpha}}{\sqrt{1-\psi_{\alpha}^2}}\right]\right\}. \tag{13}$$

The coefficients E_α, F_α and G are given in Appendix A.

In evaluating the above variables φ_α, χ_α and ψ_α the causality condition must be satisfied. That is, if R is greater than the distance travelled by the wave at the given time then the value of the variables φ_α, χ_α and ψ_α is greater than 1. In this case the terms in eqns (10)–(13) which contain that variable are put equal to zero.

Further expressions for the convoluted fundamental solutions $\tilde{U}_{ij}^{Nn}$ and $\tilde{U}_{kij}^{Nn}$ and the linear interpolation of tractions can be found in Israil and Banerjee (1990, 1991), respectively.

3.3. *Evaluation of the space integrals*

The fundamental solutions of elastodynamics are singular when $R \to 0$ and the retarded time $(t-\tau) \to 0$. The convoluted fundamental solutions, defined in the previous section, are singular during the first time step.

The kernels $\tilde{U}_{ij}^{Nn}$ and $\tilde{T}_{ij}^{Nn}$ in the displacement equation have singularities O[ln (R)] and O$(1/R)$, respectively. Integration of these types of singularities is well documented in the literature. For instance, in Dominguez (1993) $\tilde{U}_{ij}^{Nn}$ is integrated using the logarithmic Gaussian quadrature and $\tilde{T}_{ij}^{Nn}$ by using the singularity subtraction method.

In the convoluted fundamental solution $\tilde{U}_{kij}^{Nn}$ the term containing the expression $1/R\sqrt{1-\varphi_\alpha^2}$ has a singularity O$(1/R)$. The term with $\sqrt{1-\varphi_\alpha^2}/R\varphi_\alpha^2$, if considered separately, has a singularity O$(1/R^3)$. However, if the two terms corresponding to longitudinal and shear waves are added together, the singularity is reduced to O$(1/R)$.

In the convoluted fundamental solution $\tilde{T}_{kij}^{Nn}$ the term containing the expression $\sqrt{1-\varphi_\alpha^2}/R\varphi_\alpha$ has a singularity O$(1/R^2)$. The term with $(1-\varphi_\alpha^2)^{3/2}/R\varphi_\alpha^3$, if considered separately, has singularity O$(1/R^4)$. However, if the two terms corresponding to the two waves are added together, the singularity is reduced to O$(1/R^2)$. The term containing the expression $\varphi_\alpha/R\sqrt{1-\varphi_\alpha^2}$ is not singular.

From the above analysis it can be seen that the convoluted fundamental solutions have the same order of spatial singularity as the corresponding fundamental solutions of elastostatics. Both stress kernels contain the expressions $1/\sqrt{1-\varphi_\alpha^2}$, which are weakly singular at the front of the wave, i.e. when $\varphi_\alpha \to 1$. The kernels $\tilde{U}_{kij}^{Nn}$ and $\tilde{T}_{kij}^{Nn}$ can be integrated numerically using standard Gaussian quadrature, if the collocation point does not belong to the element.

For integration along an element which contains the collocation point, the integrals can be calculated using the singularity subtraction method, in a similar way to that demonstrated in elastostatics [see Portela *et al.* (1992)]. The regular part of the integrand is expressed by a Taylor expansion, of which the first few terms are subtracted from the regular part and then added back. The number of terms required in Taylor's expansion depends on the order of the singularity. The regularized part can be integrated using the standard Gaussian quadrature, while the added terms, which have a simpler form than the initial integral, can be evaluated analytically.

The first-order finite part integral can be transformed as follows:

$$\oint_{-1}^{1} \tilde{U}_{kij}^{Nn}(\xi', \xi) N^p(\xi) J^m(\xi)\, d\xi = \oint_{-1}^{1} \frac{f_{kij}(\xi)}{\xi - \xi'} d\xi = \int_{-1}^{1} \frac{f_{kij}(\xi) - f_{kij}(\xi')}{\xi - \xi'} d\xi + f_{kij}(\xi') \oint_{-1}^{1} \frac{d\xi}{\xi - \xi'}, \tag{14}$$

where $\oint$ stands for a Cauchy principal value integral and $f_{kij}(\xi)$ is the integrand of the left hand side multiplied by $(\xi - \xi')$. The first integral on the right hand side is regular and can be integrated using standard Gaussian quadrature, while the second can be evaluated analytically as

$$\oint_{-1}^{1} \frac{d\xi}{\xi - \xi'} = ln \left| \frac{1 - \xi'}{1 + \xi'} \right|. \tag{15}$$

Similarly, the second-order finite part integral can be expressed as follows:

$$\oint_{-1}^{1} \tilde{T}_{kij}^{Nn}(\xi', \xi) N^p(\xi) J^m(\xi)\, d\xi = \oint_{-1}^{1} \frac{g_{kij}(\xi)}{(\xi - \xi')^2} d\xi =$$

$$\int_{-1}^{1} \frac{g_{kij}(\xi) - g_{kij}(\xi') - g_{kij}^{(1)}(\xi')(\xi - \xi')}{(\xi - \xi')^2} d\xi + g_{kij}(\xi') \oint_{-1}^{1} \frac{d\xi}{(\xi - \xi')^2} + g_{kij}^{(1)}(\xi') \oint_{-1}^{1} \frac{d\xi}{\xi - \xi'}, \tag{16}$$

where $\oint$ stands for a Hadamard principal value integral, $g_{kij}(\xi)$ is the integrand of the left hand side multiplied by $(\xi - \xi')^2$ and $g_{kij}^{(1)}(\xi')$ denotes the first derivative of g_{kij}. The first integral of the right hand side is regular, the third integral is the same as eqn (15) above, and the second term can be evaluated as

$$\oint_{-1}^{1} \frac{d\xi}{(\xi - \xi')^2} = -\frac{2}{1 - \xi'^2}. \tag{17}$$

The application of the singularity subtraction method for one particular term is demonstrated in Appendix B.

The existence of the finite part integrals in eqns (14) and (16) requires Hölder continuity of f_{kij} and the first derivative of g_{kij} at the collocation point, respectively. Both requirements are satisfied for collocation points at internal nodes of discontinuous elements.

The coefficients c_{ij}^{l} in eqn (3) are calculated analytically [see Dominguez (1993)]. The present method requires numerical or analytical integration along one of the crack surfaces. The integrals for the opposite face can be obtained from the former, since the boundaries of the crack are coincident.

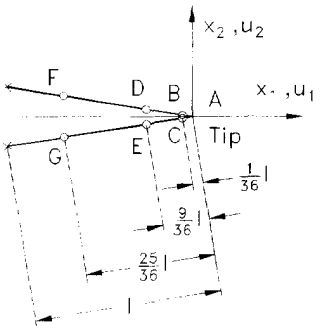

Fig. 2. Modelling of the crack using quarter-point elements.

3.4. *Matrix equation of motion*

After the discretization and integration the following matrix equation is obtained:

$$\mathbf{H}^{NN}\mathbf{u}^{N} = \mathbf{G}^{NN}\mathbf{t}^{N} + \sum_{n=1}^{N-1} (\mathbf{G}^{Nn}\mathbf{t}^{n} - \mathbf{H}^{Nn}\mathbf{u}^{n}), \tag{18}$$

where $\mathbf{u}^{n}$, $\mathbf{t}^{n}$ contain nodal values of displacements and tractions at the time step n; $\mathbf{H}^{Nn}$ and $\mathbf{G}^{Nn}$ depend on the fundamental solutions and interpolating functions. The superscripts Nn emphasize that the matrix depends on the difference between the time steps N and n. The columns of matrices $\mathbf{H}^{NN}$, $\mathbf{G}^{NN}$ are reordered according to the boundary conditions, giving new matrices $\mathbf{A}^{NN}$ and $\mathbf{B}^{NN}$. The matrix $\mathbf{A}^{NN}$ is multiplied by the vector $\mathbf{x}^{N}$ of unknown displacements and tractions and the matrix $\mathbf{B}^{NN}$ by the vector $\mathbf{y}^{N}$ of known boundary conditions, as follows:

$$\mathbf{A}^{NN}\mathbf{x}^{N} = \mathbf{B}^{NN}\mathbf{y}^{N} + \sum_{n=1}^{N-1} (\mathbf{G}^{Nn}\mathbf{t}^{n} - \mathbf{H}^{Nn}\mathbf{u}^{n}). \tag{19}$$

In each time step only the matrices which correspond to the maximum difference $N-n$ are computed. The rest of the matrices are known from the previous steps. The matrices $\mathbf{A}^{NN}$ and $\mathbf{B}^{NN}$ are calculated in the first step only since they are the same at each time step; $\mathbf{A}^{NN} = \mathbf{A}$ and $\mathbf{B}^{NN} = \mathbf{B}$. The matrix equation (19) can be written in a simpler form as

$$\mathbf{A}\mathbf{x}^{N} = \mathbf{f}^{N}, \tag{20}$$

where

$$\mathbf{f}^{N} = \mathbf{B}\mathbf{y}^{N} + \sum_{n=1}^{N-1} (\mathbf{G}^{Nn}\mathbf{t}^{n} - \mathbf{H}^{Nn}\mathbf{u}^{n}) \tag{21}$$

is a known vector. The matrix equation is solved step-by-step giving the unknown displacements and tractions at each time step. During the initial steps the fundamental solutions are non-zero only in the neighbourhood of the collocation point; they are therefore integrated only over that part of the boundary. The solution process becomes slower at later times because the vector $\mathbf{f}^{N}$ depends on all the matrices from the previous steps.

4. DYNAMIC STRESS INTENSITY FACTORS

The dynamic stress intensity factors (DSIFs) are determined using two methods: the crack opening displacements (CODs) and the path independent $\hat{J}$-integral.

4.1. *Crack opening displacements*

In order to improve the accuracy of displacements, the positions of nodes of the straight discontinuous elements adjacent to the crack tip have been changed, as shown in Fig. 2. The new distances of the pairs of nodes B–C, D–E and F–G from the crack tip A

are $\frac{1}{36}l$, $\frac{9}{36}l$ and $\frac{25}{36}l$, respectively, where l is the length of the element. The local coordinates of the nodes are the same as other discontinuous elements, i.e. $(\xi' = -\frac{2}{3}, 0, \frac{2}{3})$. For the distorted elements the local coordinate ξ is the square-root function of the distance r from the crack tip:

$$\xi = 1 - 2\sqrt{\frac{r}{l}}, \quad \text{for the crack tip at } \xi = 1, \tag{22}$$

$$\xi = -1 + 2\sqrt{\frac{r}{l}}, \quad \text{for the crack tip at } \xi = -1. \tag{23}$$

After the above modification, the displacements of the crack tip elements are approximated by a function

$$u = a_1 + a_2\sqrt{r} + a_3 r, \tag{24}$$

where a_1, a_2, a_3 are coefficients of the approximation, which depend on the displacements of nodes of the element. This type of function better represents the displacements field near the crack tip. The above modification is similar to that used for quadratic continuous quarter-point elements (QPEs) [see e.g. Blandford *et al.* (1981); Martinez and Dominguez (1984)].

The DSIFs are calculated by minimizing the sum of squared differences between the analytical and numerical values of crack opening displacements for two pairs of nodes B–C and D–E. The analytical expression Δv for the crack opening is

$$\Delta v = K\frac{\kappa + 1}{2\mu}\sqrt{\frac{2}{\pi}}\sqrt{r}, \tag{25}$$

where K is the DSIF; $\kappa = 3 - 4\nu$ for plane strain and $\kappa = (3-\nu)/(1+\nu)$ for plane stress; and ν is Poisson's ratio.

The sum of squared differences is

$$\varepsilon = (\Delta v^{BC} - \Delta u^{BC})^2 + (\Delta v^{DE} - \Delta u^{DE})^2, \tag{26}$$

where Δu denotes the numerical value of the crack opening and the superscripts the pairs of nodes.

The parameter ε can be expressed in terms of the DSIF from eqn (25). The squared difference between the numerical and analytical opening displacements, defined by ε, is a minimum if the DSIFs for mode I and mode II have the following values:

$$K_{\mathrm{I}} = \frac{6\mu}{5(\kappa+1)}\sqrt{\frac{\pi}{2l}}(\Delta u_2^{BC} + 3\Delta u_2^{DE}), \tag{27}$$

$$K_{\mathrm{II}} = \frac{6\mu}{5(\kappa+1)}\sqrt{\frac{\pi}{2l}}(\Delta u_1^{BC} + 3\Delta u_1^{DE}), \tag{28}$$

where Δu_1 and Δu_2 are the crack opening displacements along and perpendicular to the crack, respectively.

4.2. *Path independent* $\hat{J}$*-integral*

The dynamic stress intensity factors can be determined from a path independent $\hat{J}$-integral [see e.g. Kishimoto *et al.* (1980); Atluri (1986)]. For a mixed mode case the fields

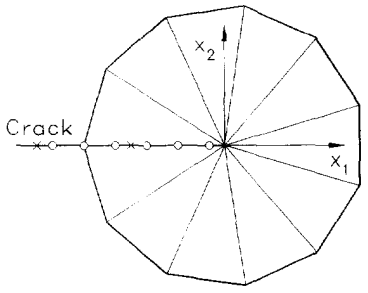

Fig. 3. Integration path for the $\hat{J}$-integral and its discretization.

of derivatives of displacements, strains, stresses, tractions and accelerations are decomposed into the symmetric mode I and the antisymmetric mode II and the $\hat{J}$-integral is calculated for the two modes of deformation as

$$\hat{J}^{\beta} = \int_{S+S_c} (W^{\beta} n_1 - t_i^{\beta} u_{i,1}^{\beta}) \, \mathrm{d}S + \int_A \rho \ddot{u}_i^{\beta} u_{i,1}^{\beta} \, \mathrm{d}A, \quad \beta = \mathrm{I}, \mathrm{II}, \tag{29}$$

where S is an arbitrary curve surrounding the crack tip; S_c are the crack surfaces; A the area enclosed by S and S_c; W the strain energy density; n_1 the component of the unit outward normal to the boundary of A; and β is the mode of deformation. The variables in eqn (29) are expressed in the local crack reference system, shown in Fig. 3. The DSIFs are calculated from the $\hat{J}^{\beta}$-integrals, as follows:

$$K_{\mathrm{I}} = \sqrt{\frac{8\mu}{\kappa+1} \hat{J}^{\mathrm{I}}} \quad \text{and} \quad K_{\mathrm{II}} = \sqrt{\frac{8\mu}{\kappa+1} \hat{J}^{\mathrm{II}}}. \tag{30}$$

The path independent integrals are calculated for a regular polygonal path with the centre at the crack tip. The first and last points of the path are the nodes on the crack faces. The domain enclosed by the path is divided into triangles. All the variables required for the $\hat{J}$-integral are obtained by using the appropriate boundary element equations. The accelerations are calculated by using the displacements at different time steps and the central difference method

$$\ddot{u}_i^N = \frac{1}{\Delta\tau^2} (u_i^{N-1} - 2u_i^N + u_i^{N+1}). \tag{31}$$

The accuracy of the above approximation depends on the variation of accelerations. A better approximation can be obtained by calculating the acceleration directly from the boundary element equation, as has been shown in Fedelinski *et al.* (1994a).

The boundary term in eqn (29) is computed using the trapezoidal rule and the domain term by using Gaussian integration.

5. NUMERICAL EXAMPLES

The present method is applied to four problems. The solutions of the first and the second problems, i.e. a pure opening mode and a mixed mode case, are obtained by using the COD and the $\hat{J}$-integral and compared with other reported solutions. The third example demonstrates an application for an infinite sheet and the fourth example a new application for a multiple crack problem. In each example the structure is instantaneously loaded by a uniform stress σ_0 at time $t = 0$. The DSIFs are normalized with respect to

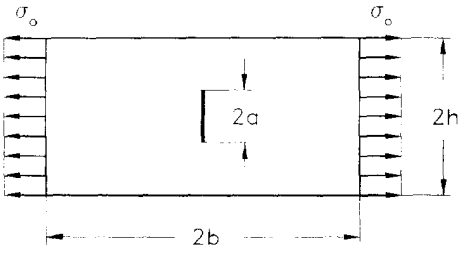

Fig. 4. Rectangular plate with a central crack.

$$K_0 = \sigma_0 \sqrt{\pi a}, \tag{32}$$

where a defines the length of the crack. The static limits are calculated using the present program and assuming a small density of the material.

5.1. *Rectangular plate with a central crack*

A rectangular plate of length $2h = 40$ mm and width $2h = 20$ mm contains a central crack of length $2a = 4.8$ mm, as shown in Fig. 4. The material properties are: the shear modulus $\mu = 76.92 \times 10^9$ Pa; Poisson's ratio $\nu = 0.3$; the density $\rho = 5000$ kg m^{-3} and the plate is under a state of plane strain. The opposite ends of the plate are loaded by the stress σ_0 with Heaviside-function time dependence. The boundary is divided into 32 boundary elements and the time step $\Delta\tau = 0.3$ μs. The use of larger numbers of elements did not alter the results by a significant amount.

The normalized DSIF K_I/K_0 is plotted in Fig. 5 and compared with that of Chen (1975), who used a finite difference method, and Aberson *et al.* (1977), who used a finite element method. In those methods a quarter of the plate was modelled. The DSIFs obtained here by the COD and the $\hat{J}$-integral are similar and in general both agree well with those results. Certain details are different, for instance the peak at $t = 4\mu$s, shown by the finite element method and the DBEM and $\hat{J}$-integral, confirmed by Lin and Ballman (1993), is not detected by the remaining methods. The use of the quarter-point element improves the DSIF results obtained from the COD, but has a negligible effect on those obtained from the $\hat{J}$-integral.

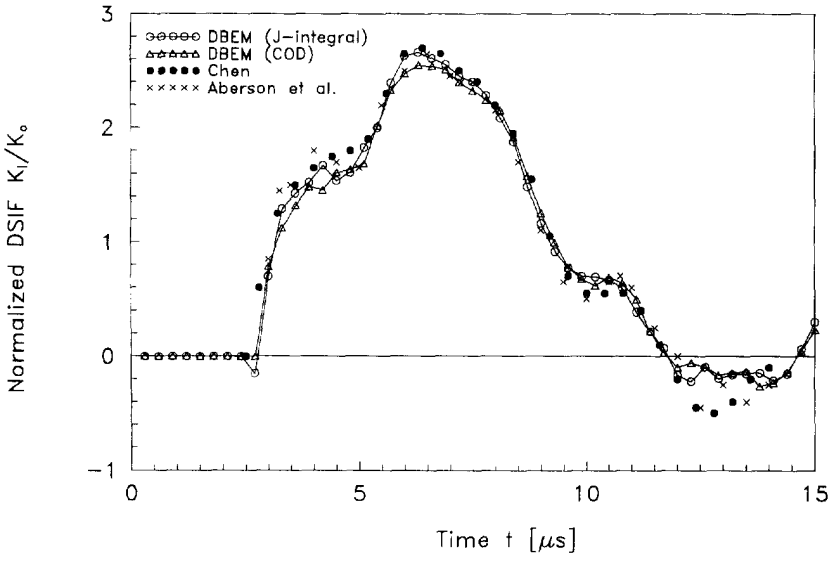

Fig. 5. Normalized dynamic stress intensity factor K_I K_0 for the rectangular plate with a central crack.

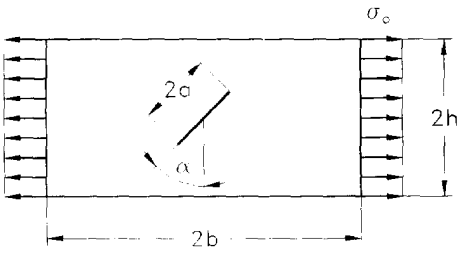

Fig. 6. Rectangular plate with an internal inclined crack.

5.2. *Rectangular plate with an internal inclined crack*

A rectangular plate of length $2b = 60$ mm and width $2h = 30$ mm contains a central inclined crack of length $2a = 14.14$ mm slanted at an angle $\alpha = 45°$, as shown in Fig. 6. The material properties are the same as in the previous example. The opposite ends of the plate are loaded by the stress σ_0. The boundary is divided into 40 boundary elements and the time step $\Delta\tau = 0.8$ μs.

The normalized DSIFs K_I/K_0 and K_{II}/K_0 are plotted in Figs 7 and 8, respectively, and compared with those of Dominguez and Gallego (1992), who used the time domain formulation and a subregion technique in the BEM, and Murti and Valliappan (1986), who used a finite element method. The DSIFs obtained here by the COD and the $\hat{J}$-integral are similar. The current results differ slightly from the reported solutions, but they agree with the results obtained using the dual reciprocity method and the DBEM [see Fedelinski *et al.* (1994a)]. The same example was solved in Fedelinski *et al.* (1994c) using the linear temporal shape function for tractions in the traction equation, and similar solutions were obtained as those presented in Figs 7 and 8.

5.3. *Two cracks at a hole in an infinite sheet*

Figure 9 shows two equal-length cracks, diametrically opposite at the edge of a circular hole of diameter $d = 20$ mm. The distance between the crack tips is $2a = 60$ mm. The material properties are: the Young's modulus $E = 0.2 \times 10^{12}$ Pa; Poisson's ratio $\nu = 0.3$; the density $\rho = 8000$ kg m^{-3}; and the plate is under a state of plane strain. The hole is loaded by a uniform normal pressure σ_0. The crack and hole boundaries are divided into a total of 44 boundary elements and the time step $\Delta\tau = 1$ μs.

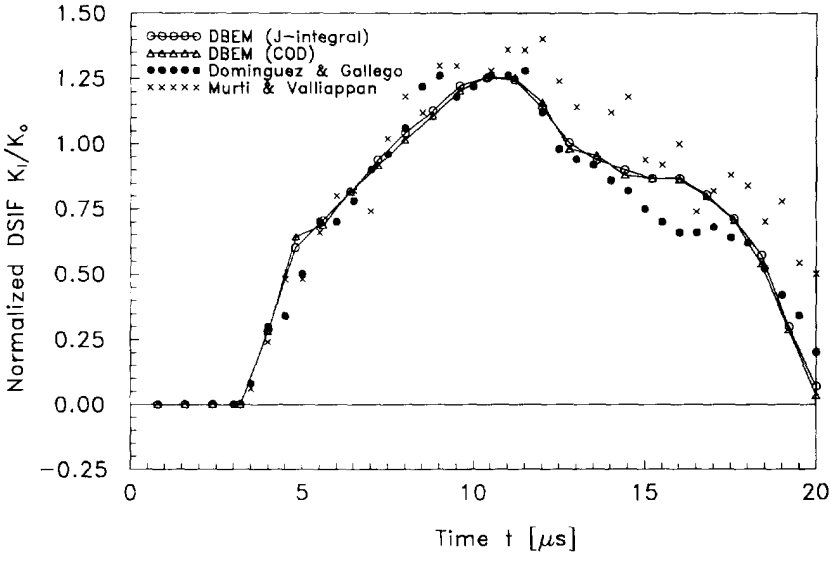

Fig. 7. Normalized dynamic stress intensity factors K_I/K_0 for the rectangular plate with an internal inclined crack.

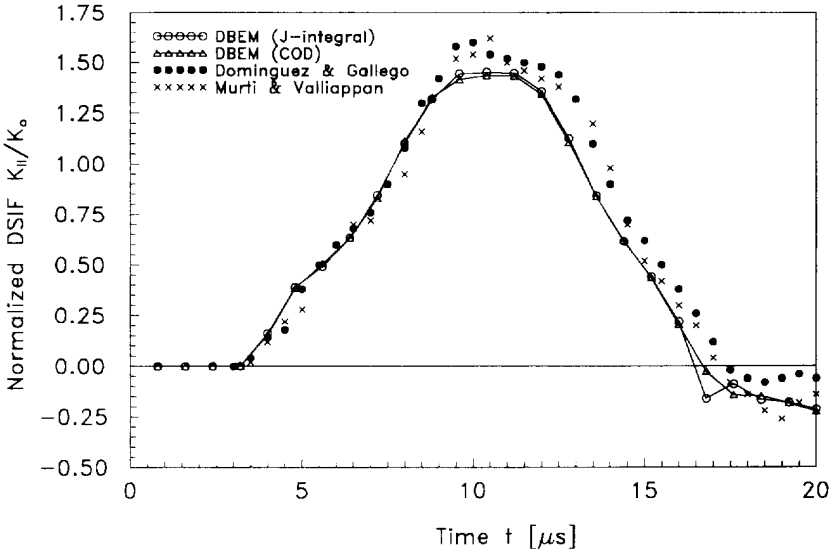

Fig. 8. Normalized dynamic stress intensity factors K_{II} K_0 for the rectangular plate with an internal inclined crack.

The normalized SIFs K_I K_0 are shown in Fig. 10. It can be seen that the DSIF tends to a static limit at long times.

5.4. *Rectangular plate with cracks at holes*

A rectangular plate of length $2b = 120$ mm and width $2h = 60$ mm contains three holes in a row of diameter $d = 10$ mm, each with two cracks, as shown in Fig. 11. The distance between the centres of holes is $w = 30$ mm. The outer holes have a pair of diametrically opposite cracks along the line of centres: the crack length a, measured from the centre of the hole, is $a = 10$ mm. The middle hole has two cracks, one of length a and the other of length $1.5a$. The material properties are the same as in the previous example. The opposite ends of the plate are loaded by the stress σ_0. The boundary is divided into 100 boundary elements and the time step $\Delta\tau = 1$ μs.

The normalized SIFs for the crack tips are plotted in Fig. 12. The largest values of both the static and the dynamic SIFs were obtained for cracks D, E and C, in that order. The static values for E and C are almost identical.

6. CONCLUSIONS

A single-region time domain boundary element method has been developed for the analysis of cracked two-dimensional structures subjected to dynamic loads. The method requires discretization of the external boundary of the body and both crack surfaces. No other discretization is required. In the subregion technique the structure is divided into

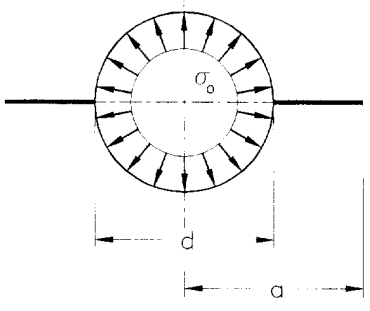

Fig. 9. Two cracks at a hole in an infinite sheet.

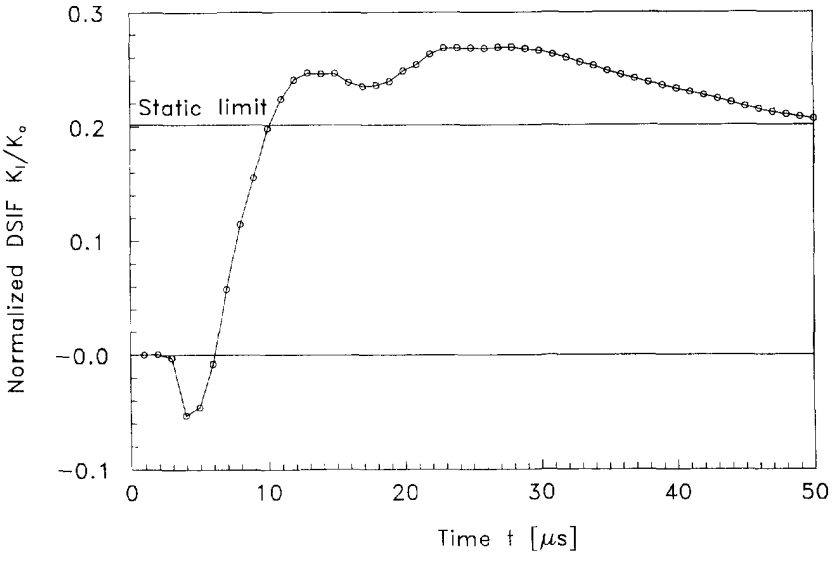

Fig. 10. Normalized dynamic stress intensity factor K_I K_o for two cracks at a hole in an infinite sheet.

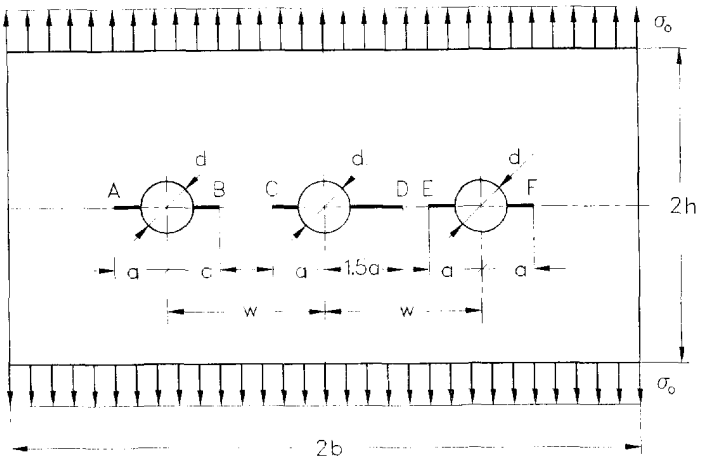

Fig. 11. Rectangular plate with cracks at holes.

subregions along continuations of crack surfaces. The artificial internal boundaries require additional elements and are inconvenient in modelling crack growth. In the displacement discontinuity method only one of the crack surfaces is discretized and the boundary integral equations are expressed in terms of the relative displacements of crack surfaces. This method needs fewer boundary elements than the present approach; however, only the relative displacements are obtained directly from the solution. The DBEM was initially combined with the dual reciprocity method. That method is less accurate than the present method since additional approximation of accelerations at internal points is used. The present method, however, is more time consuming and requires more computer memory, since in each time step two system matrices are computed and stored. The dynamic stress intensity factors were calculated from the crack opening displacements and the path independent $\tilde{J}$-integral. The solutions obtained by using these two methods are similar and agree well with other reported solutions. However, the computation of the $\tilde{J}$-integral is time consuming, since the method requires space and time integration at each time step to determine internal values.

Acknowledgement—The authors acknowledge the support of the Ministry of Defence, Defence Research Agency, under the Strategic Research Programme, Farnborough, Hants, U.K.

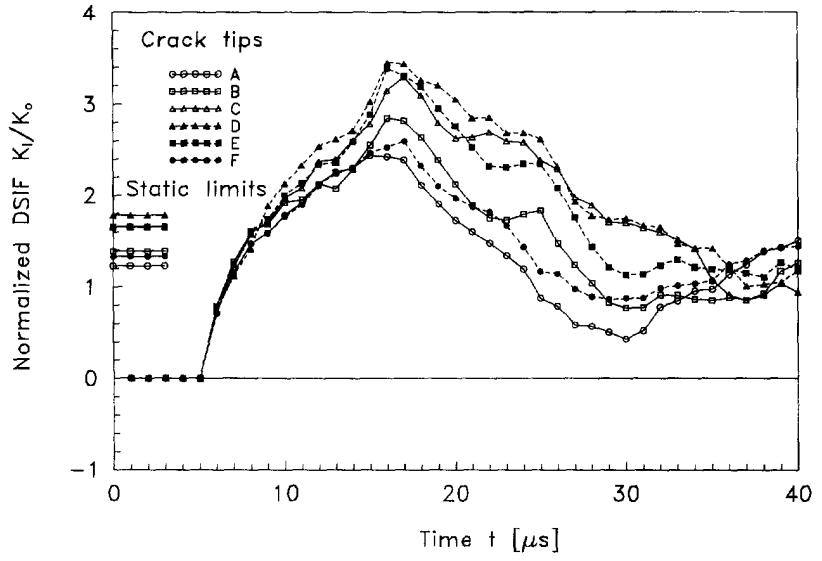

Fig. 12. Normalized dynamic stress intensity factor K_I/K_0 for the rectangular plate with cracks at holes.

REFERENCES

Aberson, J. A., Anderson, J. M. and King, W. W. (1977). Dynamic analysis of cracked structures using singularity finite elements. In *Mechanics of Fracture, Vol. 4: Elastodynamic Crack Problems* (Edited by G. C. Sih), pp. 249–294. Noordhoff International Publishing, Leyden.

Atluri, S. N. (1986). Energetic approaches and path-independent integrals in fracture mechanics. In *Computational Methods in Mechanics, Vol. 2: Computational Methods in the Mechanics of Fracture* (Edited by S. N. Atluri), pp. 121–165. North-Holland.

Blandford, G. E., Ingraffea, A. R. and Liggett, J. A. (1981). Two-dimensional stress intensity factor computations using the boundary element method. *Int. J. Num. Meth. Engng* **17**, 387–404.

Chen, Y. M. (1975). Numerical computation of dynamic stress intensity factors by a Lagrangian finite-difference method (the HEMP code). *Engng Fract. Mech.* **7**, 653–660.

Dominguez, J. and Gallego, R. (1992). Time domain boundary element method for dynamic stress intensity factor computations. *Int. J. Num. Meth. Engng* **33**(3), 635–647.

Dominguez, J. (1993). *Boundary Elements in Dynamics*. Computational Mechanics Publications, Southampton.

Fedelinski, P., Aliabadi, M. H. and Rooke, D. P. (1993). The dual boundary element method in dynamic fracture mechanics. *Engng Anal. Boundary Elem.* **12**(3), 203–210.

Fedelinski, P., Aliabadi, M. H. and Rooke, D. P. (1994a). The dual boundary element method: $\hat{J}$-integral for dynamic stress intensity factors. *Int. J. Fract.* **65**(4), 369–381.

Fedelinski, P., Aliabadi, M. H. and Rooke, D. P. (1994b). The dual boundary element method for dynamic analysis of cracked pin-loaded lugs. In *Localized Damage III, Computer Aided Assessment and Control* (Edited by M. H. Aliabadi *et al.*), pp. 571–578. Computational Mechanics Publications, Southampton.

Fedelinski, P., Aliabadi, M. H. and Rooke, D. P. (1994c). Dynamic stress intensity factors in mixed-mode: time-domain formulation. In *Boundary Elements XVI* (Edited by C. A. Brebbia), pp. 513–520. Computational Mechanics Publications, Southampton.

Freund, L. B. (1990). *Dynamic Fracture Mechanics*. Cambridge University Press, Cambridge.

Gallego, R. and Dominguez, J. (1992). Dynamic crack propagation analysis by moving singular boundary elements. *J. Appl. Mech. Trans. ASME* **59**, 158–162.

Hirose, S. (1989). Scattering from an elliptic crack by the time-domain boundary integral equation method. In *Advances in Boundary Elements, Vol. 3: Stress Analysis* (Edited by C. A. Brebbia and J. J. Connor), pp. 99–110. Computational Mechanics Publications, Southampton.

Hirose, S. and Achenbach, J. D. (1988). Application of BEM to transient analysis of a 3-D crack. In *Boundary Element Methods in Applied Mechanics* (Edited by M. Tanaka and T. A. Cruse), pp. 255–264. Pergamon Press.

Hirose, S. and Achenbach, J. D. (1989). Time-domain boundary element analysis of elastic wave interaction with a crack. *Int. J. Num. Meth. Engng* **28**(3), 629–644.

Hirose, S. and Achenbach, J. D. (1991). Acoustic emission and near-tip elastodynamic fields of a growing penny-shaped crack. *Engng Fract. Mech.* **39**(1), 21–36.

Israil, A. S. M. and Banerjee, P. K. (1990). Two-dimensional transient wave-propagation problems by time-domain BEM. *Int. J. Solids Structures* **26**,(8), 851–864.

Israil, A. S. M. and Banerjee, P. K. (1991). Interior stress calculations in 2-D time-domain transient BEM analysis. *Int. J. Solids Structures* **27**(7), 915–927.

Kishimoto, K., Aoki, S. and Sakata, M. (1980). Dynamic stress intensity factors using $\hat{J}$-integral and finite element method. *Engng Fract. Mech.* **13**, 387–394.

Lin, X. and Ballmann, J. (1993). Re-consideration of Chen's problem by finite difference method. *Engng Fract. Mech.* **44**(5), 735–739.

Manolis, G. D. and Beskos, D. E. (1988). *Boundary Element Methods in Elastodynamics*. Unwin Hyman, London.

Martinez, J. and Dominguez, J. (1984). On the use of quarter-point boundary elements for stress intensity factor computations. *Int. J. Num. Meth. Engng* **20**(10), 1941–1950.
Mettu, S. R. and Nicholson, J. W. (1988). Computation of dynamic stress intensity factors by the time domain boundary integral equation method—II. Examples. *Engng Fract. Mech.* **31**(5), 769–782.
Mettu, S. R. and Kim, K. S. (1991). An application of the time-domain boundary integral equation method to dynamic crack propagation. *Engng Fract. Mech.* **39**(2), 339–345.
Mi, Y. and Aliabadi, M. H. (1992). Dual boundary element method for three-dimensional fracture mechanics analysis. *Engng Anal. Boundary Elem.* **10**(2), 161–171.
Mi, Y. and Aliabadi, M. H. (1994). Three-dimensional crack growth simulation using BEM. *Comput. Struct.* **52**(5), 871–878.
Murti, V. and Valliappan, S. (1986). The use of quarter point element in dynamic crack analysis. *Engng Fract. Mech.* **23**(3), 585–614.
Nicholson, J. W. and Mettu, S. R. (1988). Computation of dynamic stress intensity factors by the time domain boundary integral equation method—I. Analysis. *Engng Fract. Mech.* **31**(5), 759–767.
Nishimura, N., Guo, Q. C. and Kobayashi, S. (1987). Boundary integral equation methods in elastodynamic crack problems. In *Boundary Elements IX, Vol. 2: Stress Analysis Applications* (Edited by C. A. Brebbia, W. L. Wendland and G. Kuhn), pp. 279–291. Computational Mechanics Publications, Springer-Verlag.
Nishimura, N., Guo, Q. C. and Kobayashi, S. (1988). Elastodynamic crack analysis by BIEM. In *Boundary Element Methods in Applied Mechanics* (Edited by M. Tanaka and T. A. Cruse), pp. 245–254. Pergamon Press.
Portela, A., Aliabadi, M. H. and Rooke, D. P. (1992). The dual boundary element method: effective implementation for crack problems. *Int. J. Num. Meth. Engng* **33**(6), 1269–1287.
Portela, A., Aliabadi, M. H. and Rooke, D. P. (1993). Dual boundary element incremental analysis of crack propagation. *Comput. Struct.* **46**(2), 237–247.
Sih, G. C. (ed.) (1977). *Mechanics of Fracture, Vol. 4: Elastodynamic Crack Problems*. Noordhoff International Publishing, Leyden.
Zhang, Ch. and Achenbach, J. D. (1989). Time-domain boundary element analysis of dynamic near-tip fields for impact-loaded collinear cracks. *Engng Fract. Mech.* **32**(6), 899–909.
Zhang, Ch. and Gross, D. (1993). A non-hypersingular time-domain BIEM for 3-D transient elastodynamic crack analysis. *Int. J. Num. Meth. Engng* **36**(17), 2997–3017.

APPENDIX A

The coefficients of the convoluted fundamental solution $\tilde{T}_{ij}^{Nn}$ in eqn (11) are [see Israil and Banerjee (1990)]:

$$A_\alpha = -(-1)^\alpha\left[n_j R_{,i} + n_i R_{,j} + \frac{\partial R}{\partial n}(\delta_{ij} - 4R_{,i}R_{,j})\right], \tag{A1}$$

$$B_1 = \frac{\lambda}{\mu} n_j R_{,i} + 2\frac{\partial R}{\partial n} R_{,i}R_{,j}, \tag{A2}$$

$$B_2 = \frac{\partial R}{\partial n}(\delta_{ij} - 2R_{,i}R_{,j}) + n_i R_{,j}, \tag{A3}$$

where n_i is the component of the outward normal at the boundary and λ is the Lame constant.

The coefficients of the convoluted fundamental solution $\tilde{U}_{kij}^{Nn}$ in eqn (12) are [see Israil and Banerjee (1991)]:

$$C_1 = \frac{\lambda}{\mu}\delta_{ij}R_{,k} + 2R_{,i}R_{,j}R_{,k}, \tag{A4}$$

$$C_2 = 2R_{,i}R_{,j}R_{,k} - R_{,i}\delta_{jk} - R_{,j}\delta_{ik}, \tag{A5}$$

$$D = R_{,i}\delta_{jk} + R_{,j}\delta_{ik} + R_{,k}\delta_{ij} - 4R_{,i}R_{,j}R_{,k}. \tag{A6}$$

The coefficients of the convoluted fundamental solution $\hat{T}_{kij}^{Nn}$ in eqn (13) are [see Israil and Banerjee (1991)]:

$$E_1 = \left(\frac{\lambda}{\mu}\delta_{ij} + 2R_{,i}R_{,j}\right)\left(\frac{\lambda}{\mu}n_k + 2\frac{\partial R}{\partial n}R_{,k}\right), \tag{A7}$$

$$E_2 = \frac{\partial R}{\partial n}(4R_{,i}R_{,j}R_{,k} - R_{,i}\delta_{jk} - R_{,j}\delta_{ik}) - n_i R_{,j}R_{,k} - n_j R_{,i}R_{,k}, \tag{A8}$$

$$F_1 = -n_k\left[\frac{\lambda}{\mu}\delta_{ij}\left(2 + \frac{\lambda}{\mu}\right) + 2R_{,i}R_{,j}\right] - 2n_i R_{,j}R_{,k} - 2n_j R_{,i}R_{,k} - 2\frac{\partial R}{\partial n}(R_{,i}\delta_{jk} + R_{,j}\delta_{ik} + R_{,k}\delta_{ij} - 6R_{,i}R_{,j}R_{,k}), \tag{A9}$$

$$F_2 = n_i(\delta_{jk} - 2R_{,j}R_{,k}) + n_j(\delta_{ik} - 2R_{,i}R_{,k}) - 2n_k R_{,i}R_{,j} - 2\frac{\partial R}{\partial n}(R_{,i}\delta_{jk} + R_{,j}\delta_{ik} + R_{,k}\delta_{ij} - 6R_{,i}R_{,j}R_{,k}), \tag{A10}$$

$$G = n_i(-\delta_{jk}+4R_{,j}R_{,k})+n_j(-\delta_{ik}+4R_{,i}R_{,k})+n_k(-\delta_{ij}+4R_{,i}R_{,j})+4\frac{\partial R}{\partial n}(R_{,i}\delta_{jk}+R_{,j}\delta_{ik}+R_{,k}\delta_{ij}-6R_{,i}R_{,j}R_{,k}).$$

APPENDIX B

The application of the singularity subtraction method is demonstrated here for just one particular term of the convoluted fundamental solution $\tilde{T}^{Nn}_{kij}$ in eqn (13); this term can be written as:

$$I_1 = \int_{-1}^{1} \frac{(-1)^2\mu^2}{2\pi\rho c_\alpha^2}\frac{1}{R(\xi)c_\alpha\Delta\tau}2(E_\alpha+F_\alpha)\frac{\sqrt{1-\varphi_\alpha^2(\xi)}}{\varphi_\alpha(\xi)}N^p(\xi)J^m(\xi)\,d\xi, \tag{B1}$$

which has singularity $O(1/R^2)$. The coefficients E_α and F_α are independent of ξ for a straight element. The above expression can be written as $I_1 = CI_2$, where C is a constant and I_2 contains all the spatial dependence and is of the form

$$I_2 = \int_{-1}^{1} \frac{\sqrt{1-[aR(\xi)]^2}}{R^2(\xi)}N^p(\xi)J^m(\xi)\,d\xi, \tag{B2}$$

where

$$a = \frac{1}{c_\alpha\Delta\tau(N-n+1)}. \tag{B3}$$

The spatial quadratic shape function $N^p(\xi)$ can be written in a general form as

$$N^p(\xi) = b\xi^2+c\xi+d, \tag{B4}$$

where b, c and d are constants.

Consider the integration of I_2 along the quarter-point element, when the crack tip has the coordinate $\xi = -1$. For this element the Jacobian is

$$J^m(\xi) = \tfrac{1}{2}l(\xi+1), \tag{B5}$$

and the distance $R(\xi)$ between the source point ξ' and the field point ξ is

$$R(\xi) = \tfrac{1}{4}l(\xi-\xi')(\xi+\xi'+2). \tag{B6}$$

Substituting eqns (B4), (B5) and (B6) into eqn (B2) we obtain

$$I_2 = \int_{-1}^{1} \frac{\sqrt{1-[a\frac{1}{4}l(\xi-\xi')(\xi+\xi'+2)]^2}}{[\frac{1}{4}l(\xi-\xi')(\xi+\xi'+2)]^2}(b\xi^2+c\xi+d)\tfrac{1}{2}l(\xi+1)\,d\xi. \tag{B7}$$

Therefore, function $g_{kij}(\xi)$ in eqn (16) is

$$g_{kij}(\xi) = \frac{\sqrt{1-[a\frac{1}{4}l(\xi-\xi')(\xi+\xi'+2)]^2}}{[\frac{1}{4}l(\xi+\xi'+2)]^2}(b\xi^2+c\xi+d)\tfrac{1}{2}l(\xi+1), \tag{B8}$$

and the terms required for the Taylor expansion in eqn (16) are

$$g_{kij}(\xi') = \frac{2(b\xi'^2+c\xi'+d)}{l(\xi'+1)}, \tag{B9}$$

$$g^{(1)}_{kij}(\xi') = \frac{2(2b\xi'+c)}{l(\xi'+1)}. \tag{B10}$$

The other terms of the convoluted fundamental solutions can be treated in a similar way.